Journal of Marine Science and Technology

Volume 26 | Issue 5 Article 11

CHANGING FLOW CAPACITY IN THE UPPER YELLOW RIVER BY USING A STANDARDIZED DIKE

Tao Bai
State Key Laboratory of Eco-hydraulics in Northwest Arid Region of China, Xi'an University of Technology, Xi'an, Shaanxi, China, baitao@xaut.edu.cn

Jian Wei
State Key Laboratory of Eco-hydraulics in Northwest Arid Region of China, Xi'an University of Technology, Xi'an, Shaanxi, China

Rong Ma
Hanjiang-to-Weihe River Valley Water Diversion Project Construction Co., Ltd., Shaanxi Province, Xi'an, Shaanxi, China.

Chuan-Hui Ma
State Key Laboratory of Eco-hydraulics in Northwest Arid Region of China, Xi'an University of Technology, Xi'an, Shaanxi, China.

Qiang Huang
State Key Laboratory of Eco-hydraulics in Northwest Arid Region of China, Xi'an University of Technology, Xi'an, Shaanxi, China

Follow this and additional works at: https://jmstt.ntou.edu.tw/journal

Part of the Engineering Commons

Recommended Citation

Bai, Tao; Wei, Jian; Ma, Rong; Ma, Chuan-Hui; and Huang, Qiang (2018) "CHANGING FLOW CAPACITY IN THE UPPER YELLOW RIVER BY USING A STANDARDIZED DIKE," *Journal of Marine Science and Technology*: Vol. 26: Iss. 5, Article 11.
DOI: 10.6119/JMST.201810_26(5).0011
Available at: https://jmstt.ntou.edu.tw/journal/vol26/iss5/11

This Research Article is brought to you for free and open access by Journal of Marine Science and Technology. It has been accepted for inclusion in Journal of Marine Science and Technology by an authorized editor of Journal of Marine Science and Technology.

CHANGING FLOW CAPACITY IN THE UPPER YELLOW RIVER BY USING A STANDARDIZED DIKE

Acknowledgements

This study is supported by the National Key R & D Program of China (2017YFC0405900); Planning Project of Science and Technology of Water Resources of Shaanxi (2017slkj-16, 2017slkj-27); the China Postdoctoral Science Foundation (2017M623332XB); and the Basic Research Plan of Natural Science in Shaanxi Province (2018JQ5145). The authors are indebted to the reviewers for their valuable comments and suggestions.

This research article is available in Journal of Marine Science and Technology: https://jmstt.ntou.edu.tw/journal/vol26/iss5/11

Journal of Marine Science and Technology, Vol. 26, No. 5, pp. 721-730 (2018)
DOI: 10.6119/JMST.201810_26(5).0011

CHANGING FLOW CAPACITY IN THE UPPER YELLOW RIVER BY USING A STANDARDIZED DIKE

Tao Bai[1], Jian Wei[1], Rong Ma[2], Chuan-Hui Ma[1], and Qiang Huang[1]

Key words: bankfull flow, flow capacity, safety design flow, standardized dike.

ABSTRACT

The flow capacity of the Ningxia-Inner Mongolia reach of the Yellow River has declined substantially for the effects of reservoir regulation, higher concentration of channel sedimentation, reduced upstream inflow, and increased demand for water resources downstream. This has resulted in frequent flooding and ice-related incidents, which severely threaten downstream safety. Accordingly, this paper proposes flow-capacity limitations on the basis of a standardized dike design to acquire optimal safety overflow for the upstream of Yellow River. First, historical data (1946-2012) from six hydrological stations (S1-S6) are collected, and flow capacities covering 1965-2006 (Data 1) and 2007-2010 (Data 2) are compared. Second, flow-capacity models based on standardized dikes are established for the studied river stretch (Data 3: 2011-2012) and solved using three methods: water level and flow relationships (MD1), velocity-area method (MD2), and Manning resistance equation (MD3). Third, the applicability of the models is verified. The results indicate that MD1 is consistently superior to MD2 and MD3. Last, this study determines that using MD1 with standardized dikes can increase the maximum flow at S3, S5, and S6 in the Ningxia-Inner Mongolia reaches to 8,920, 9,000, and 8,290 m^3/s, respectively. The paper contributes to water and sediment regulation in the Ningxia-Inner Mongolia reaches, with pivotal practical approaches for improving the flood-discharge capacity and constructing standardized dikes in the Ningxia-Inner Mongolia reaches of the upper Yellow River.

I. INTRODUCTION

The Yellow River, known as the "Mother River" of China, originates in the Qinghai-Tibet Plateau and flows through nine Chinese provinces with basin area of 750,000 km^2 and annual runoff of 58 billion m^3. Passing through the Maowusu Desert, the Ningxia-Inner Mongolia reaches, locate at Ningxia and Inner Mongolia provinces in the upper Yellow River, are the northernmost of the Yellow River. The distribution of the main hydrological stations (S1-S6) is shown in Fig. 1. In recent years, affected by reservoir regulation, reduced inflow, and increased water pumping, water supply in the Ningxia-Inner Mongolia reach has sharply decreased (Fig. 2). Additionally, channel shrinkage and sedimentation have caused the formation of suspended river sediments, both in tributaries and the main stream (Chang et al., 2012; Bai et al., 2017), causing frequent flooding and ice disasters even in small flows. The excessively low flow capacity poses a severe threat of flood and ice-flood safety, which is exacerbated by water bottlenecks and sediment regulation in the Ningxia-Inner Mongolia reach.

Many studies have investigated flow capacity (Chen et al., 2007; Wu et al., 2008; Xia et al., 2010), labyrinth side weirs (Emiroglu et al., 2010), and straight compound channels (Unal et al., 2010) in the lower Yellow River. Linear genetic programming (Azamathulla et al., 2012), the adaptive neuro-fuzzy technique (Emiroglu et al., 2010; Unes et al., 2015), artificial neural network approach (Tayfur et al., 2011), and slope-area method (Kordi et al., 2011) have been used to predict and estimate flow. However, few studies have investigated the flow capacity of the Ningxia-Inner Mongolia reach of the upper Yellow River. Accordingly, flow capacity based on a standardized dike is proposed to achieve optimal safety overflow for the Yellow River in this paper. Dikes with a specified form and surface material that can satisfy the flood-control standards of the channel and surrounding settlements are referred to as standardized dikes.

As shown in Fig. 3, the flow capacity of the Ningxia-Inner Mongolia reach is investigated in this study to determine the current flows of each of its sections, the reason for the decreased flow capacity, and the optimal safety overflow for each of its sections by using standardized dikes.

Data from six hydrological stations (S1-S6) covering the years 1946-2012 were collected to elucidate the reasons for reduced flow capacity and determine contemporary flow capa-

Paper submitted 09/12/17; revised 02/01/18; accepted 09/20/18. Author for correspondence: Tao Bai (e-mail: baitao@xaut.edu.cn).
[1] *State Key Laboratory of Eco-hydraulics in Northwest Arid Region of China, Xi'an University of Technology, Xi'an, Shaanxi, China.*
[2] *Hanjiang-to-Weihe River Valley Water Diversion Project Construction Co., Ltd., Shaanxi Province, Xi'an, Shaanxi, China.*

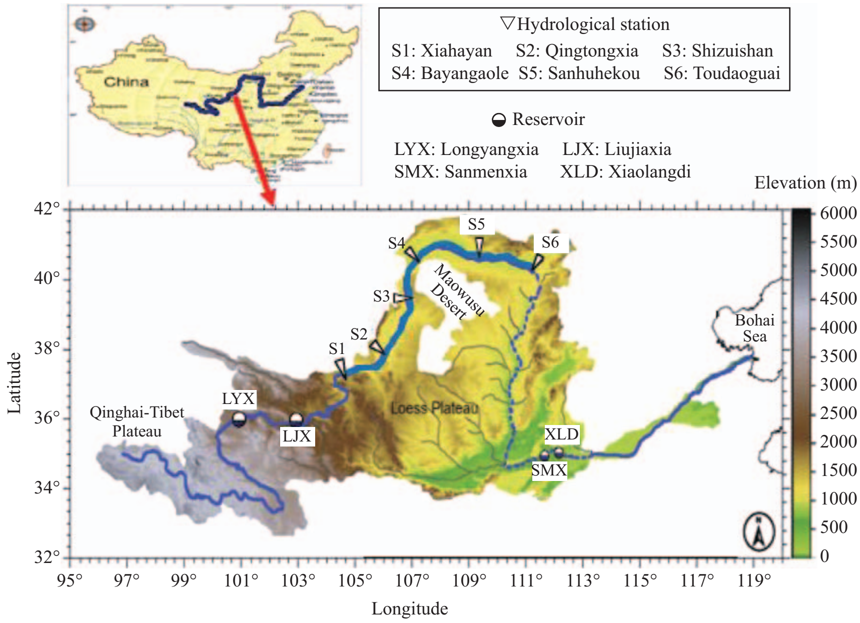

Fig. 1. Drainage basin map of the Yellow River, with the locations of major hydrological stations and reservoirs. The dotted line represents the middle Yellow River, which divides the Yellow River into the upper Yellow River (upper S6) and the lower Yellow River. The thick blue line represents the Ningxia-Inner Mongolia reach of the upper Yellow River.

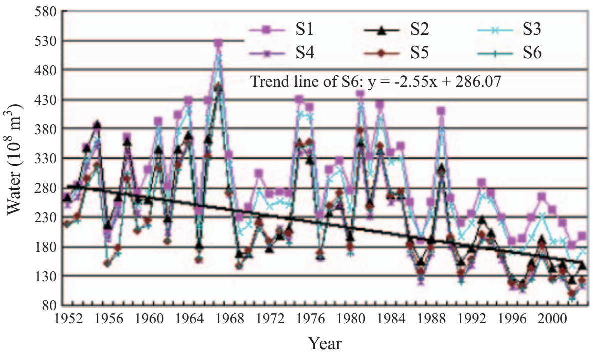

Fig. 2. Water change process and trends of hydrological stations (S1-S6) from 1952 to 2006.

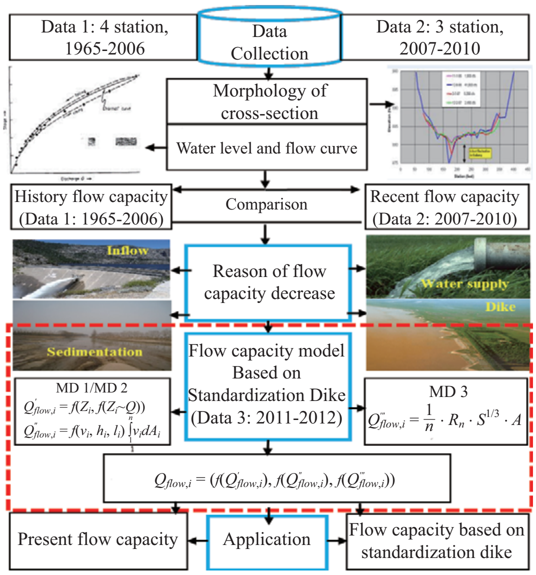

Fig. 3. Flowchart and key techniques.

city. This study used three methods to estimate river flow and established flow-capacity models based on standardized dikes along the studied section of the river, enabling us to determine the present flow capacity and that based on standardized dikes at the main hydrological stations in the Ningxia-Inner Mongolia reach. On the basis of the research findings, we propose optimal safety overflow choices that can support flood-control and water and sediment regulation.

II. SUMMARY OF DATA

There are six principal hydrological stations (S1-S6) in the Ningxia-Inner Mongolia reach of the upper Yellow River (Fig. 1). In this paper, two factors, the (1) morphology of the cross-section and (2) relationship between water level and flow, are used to describe each section's flow capacity. Longitudinal data are collected, and the measured characteristics are listed in Table 1, which include water level, flow, water, the morphology of the cross-section, area and width of the water surface, water depth, and flow velocity. The data on the morphology of the cross-section for each section are measured at least once every year, with more than 70 sets of start-point distance, water level, water surface area, water surface width, and water depth data. Flow data are measured twice daily. Moreover, several pieces of dike-related data are collected, including dike position, start-point distance, and elevation. Data such as timescale, data length, and data number are presented in Table 1. The total number of

Table 1. Characteristics and form of collected data.

Data name (unit)	Length	Timescales	Station	Number
Water (10^8 m^3)	1952-2006	year	S1-S6	330
Water level (m)	1946-2012	daily	S1-S6	146730
Flow (m^3/s)	1946-2012	daily	S1-S6	146730
Start point distance and elevation (m)	1965-2012 1965-1997	1 time/year	S1, S3, S5, S6 S2	31500
Water surface area (m^2)	1965-2012 1965-1997	1 time/year	S1, S3, S5, S6 S2	31500
Water surface width (m)	1965-2012 1965-1997	1 time/year	S1, S3, S5, S6 S2	31500
Water depth (m)	1965-2012 1965-1997	1 time/year	S1, S3, S5, S6 S2	31500
Flow velocity (m/s)	1965-2012	daily	S1-S6	20160
Sedimentation (10^8 t/year)	1952-2006	year	S1-S6	330

Table 2. Measured extreme value for water level and flow for each section from 1946 to 2006.

Section name	Maximum water level (m)	Corresponding flow (m^3/s)	Occurrence time (month/day/year)	Maximum flow (m^3/s)	Corresponding water level (m)	Occurrence time (month/day/year)
S1	1235.19	5770	09/16/1981	5770	1235.19	09/16/1981
S2	1138.87	5710	09/17/1981	6230	1139.42	09/16/1946
S3	1092.35	5820	09/18/1946	5820	1092.35	09/18/1946
S4	1054.40	5500	12/06/1993	5290	1052.03	09/19/1981
S5	1020.81	772	03/03/2006	5400	1019.94	09/22/1981
S6	990.69	5310	09/21/1967	5310	990.69	09/21/1967

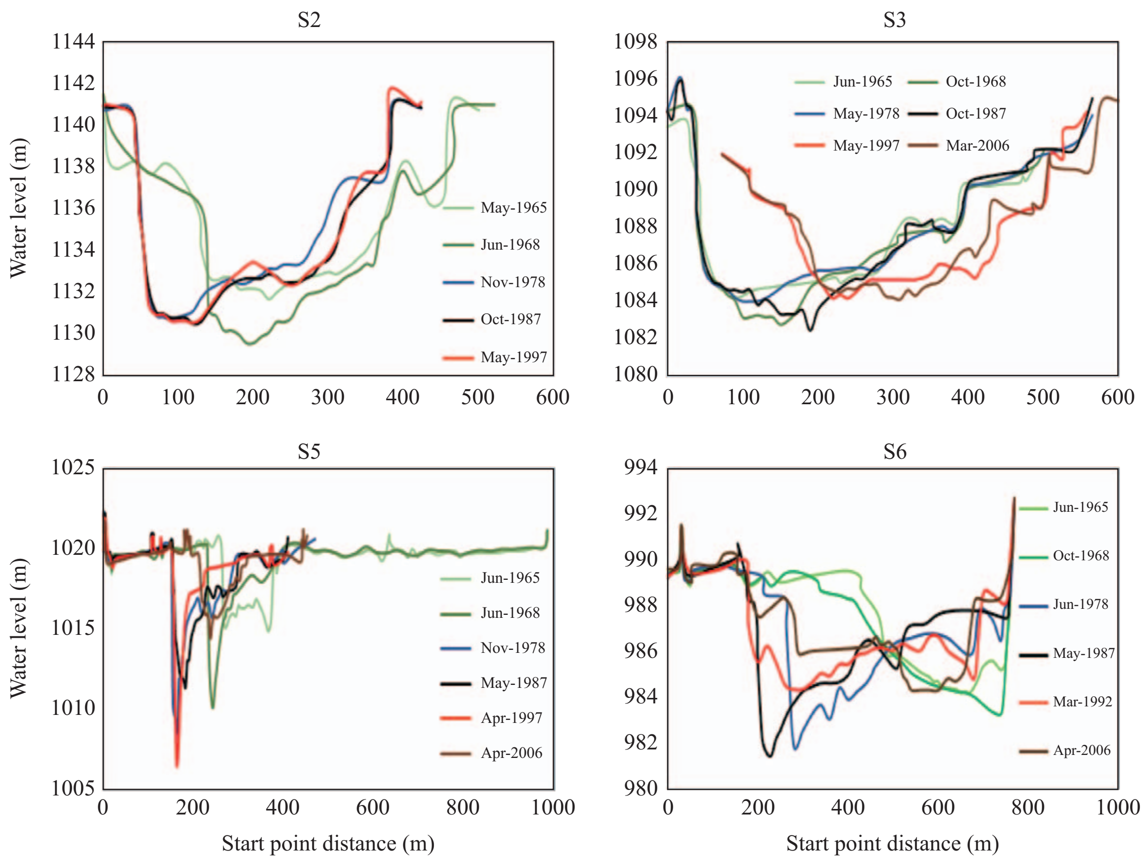

Fig. 4. Historical typical morphologies of the cross-section process from 1965 to 2006.

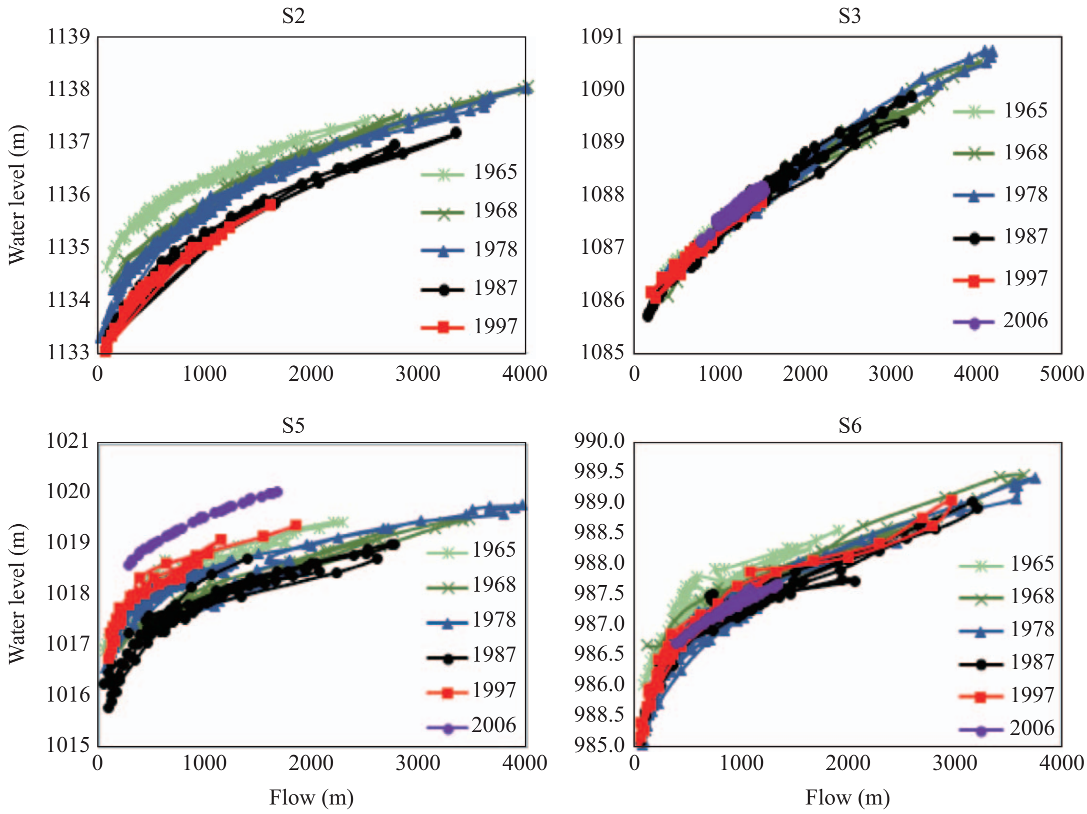

Fig. 5. Historical water levels and flow-relationship curves from 1965 to 2006.

data points exceeds 0.44 million.

III. FLOW-CAPACITY ANALYSIS

1. Historical Flow Capacity

The data series from the hydrological stations are divided into three periods: pre-2006 (historical data, Data 1), 2007-2010 (recent data, Data 2) and 2011-2012 (current data, Data 3). The historical data illustrate flow capacity over the past 40 years (Table 2; Fig. 4). The maximum flow at S5 in 2006 was 772 m^3/s, a sharp decrease relative to that in 1981.

Fig. 4 shows clearly that the typical historical morphology of the cross-section at each station has changed; this includes not only the width and depth of the channel but also the width and depth of the riverbed. For example, the width of the riverbed at S5 decreased by 40% from 2.5 km to less than 1.5 km, and the maximum depth of the riverbed decreased by more than half, from 10 m to less than 5 m. The severe reduction in the cross-section morphology and flow area in S5 may explain the substantial reduction in its flow capacity.

Fig. 5 presents the water-level and flow-relationship curve from 1965 to 2006 and accurately depicts the flow capacity. Compared with the flow range (3,800-4,200 m^3/s) before 1978, that in 2006 was less than 2,000 m^3/s. Moreover, the flow-relationship curve exhibited a downward trend before 1987 and a common upward trend between 1997 and 2006. For example, from 1987 to 2006, the water level at S5 increased by 2 m when the flow was 1000 m^3/s, and the flow decreased from more than 4,000 m^3/s to less than 1,000 m^3/s when the water level was 1,019 m.

2. Recent Flow Capacity

The Data 2 (2007-2010) dataset characterizes flow capacity over this 4-year period, as shown in Fig. 6. In line with the historical trends (Figs. 4 and 5), the width and depth of the cross-section morphology were narrower and shallower each year, and the flow area gradually decreased. The flow range decreased to less than 1500 m^3/s at S6.

3. Flow Capacity Comparison and Reasons

To compare the historical flow capacity with recent flow capacity, we selected the maximum width, depth, and flow area of the channel, as well as maximum flow and range of the water level, for 1965-2006 and 2010 (Table 3). The cross-section morphology at S5 changed substantially, with the maximum channel width and flow area decreasing by 54.0% and 50.6%, respectively, and the riverbed elevation increasing by 4.1 m (35.2%). Moreover, the cross-section morphology of S3 continued to shrink, and the flow area decreased by 15.1%. The flow at S3, S5, and S6 during 2007-2010 was less than 2,000 m^3/s, decreasing by 57.6%, 56.6%, and 64.7%, respectively, between 1965 and 2006. Overall, compared with the period 1965-2006, the width, depth, and flow area of the cross-section decreased in the period

Table 3. Cross-section morphology and flow comparison results.

Station	Decrease value				Decrease proportion			
	Width (m)	Depth (m)	flow area (m^2)	Flow (m^3/s)	Width (%)	Depth (%)	flow area (%)	Flow (%)
S3	122.0	3.4	543.9	2412	21.6	25.2	15.1	57.6
S5	1382.4	4.1	1757.6	2240	54.0	35.2	50.6	56.6
S6	34.0	1.0	334.6	2432	4.1	10.1	10.4	64.7

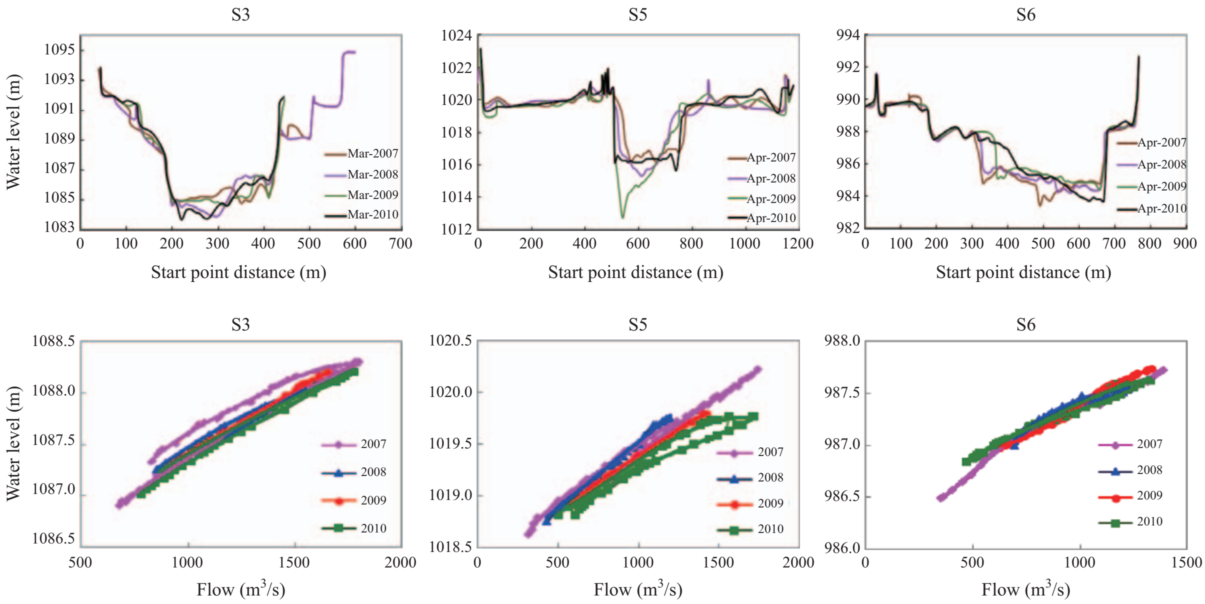

Fig. 6. Recent morphology and water level and flow relationship curves from 2007 to 2010.

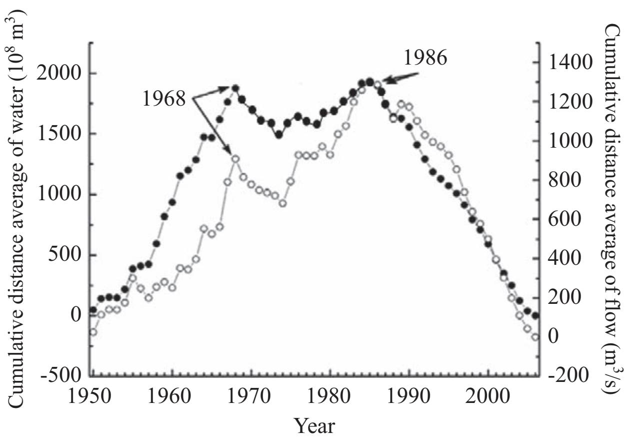

Fig. 7. Cumulative average distance of water and flow at S6.

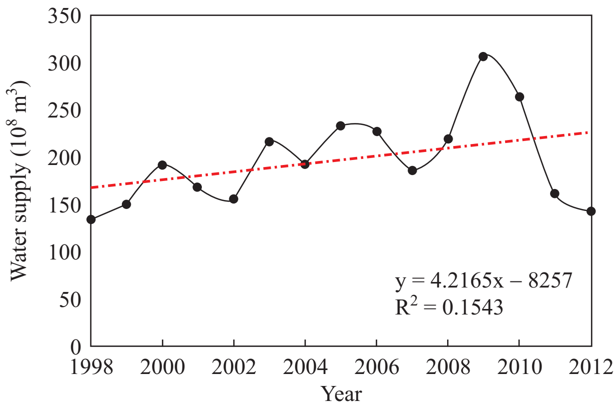

Fig. 8. Total water supply of the Yellow River.

2007-2010, especially at S5. Although the flow-relationship curves gradually stabilized, the flow capacity during 2007-2010 continued to exhibit a decreasing trend.

The reasons for the decrease in flow capacity are considered from four aspects in this paper: inflow, water supply, sedimentation, and dikes.

Inflow is a key factor in reduced flow capacity. Fig. 2 illustrates that the inflow at each section exhibits a decreasing trend from 1952 to 2010. Catastrophic points in the accumulative anomaly curve of water and flow at S6 occurred in 1968 and 1986 (Ran et al., 2010), which were caused by initial use of the LJX and LYX reservoirs, respectively, as presented in Fig. 7. This demonstrates that inflow at S1-S6 was strongly influenced by the operation of the LYX and LJX reservoirs.

Driven by population growth, socioeconomic development (Chang et al., 2013), the growth of irrigated areas (Fu et al., 2004), and increased water demands (Fig. 8), increasing amounts

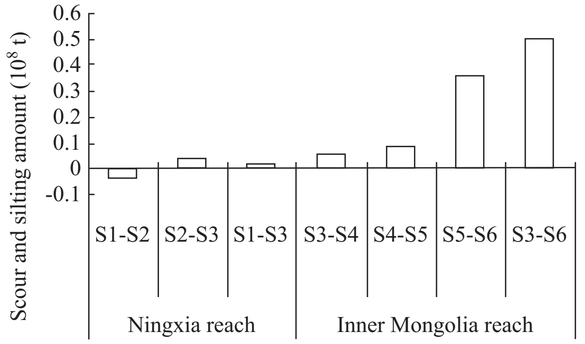

Fig. 9. Amount of scour and silt of the upper Yellow River.

of water are pumped from the Yellow River. Thus, the water remaining in the river has decreased sharply. Moreover, because the population, industrial activity, and irrigation areas are likely to increase (Xu et al., 2002), even greater amounts of water will be required. Thus, water in the Yellow River will become even scarcer. Therefore, the decreased inflow in the upper Yellow River and increased water pumping will deplete the river's water supply, and the energy will be insufficient to flush the river. Thus, silt will remain, resulting in riverbed elevation. Consequently, the area of the cross-section will be reduced, and the flow capacity will in turn decrease further.

Furthermore, decreased flow capacity in the Ningxia-Inner Mongolia reach is directly affected by sedimentation. Fig. 9 presents the amount of scour and silt in the Ningxia-Inner Mongolia reach of the upper Yellow River during 1952-2006. As Fig. 9 indicates, in addition to the S1-S2 channel, the S2-S6 channel is clearly silted, especially the S5-S6 channel. According to the Yellow River Sediment Bulletin, more than 5 billion kilograms of sediment is deposited in the Ningxia-Inner Mongolia reach annually, especially between S5-S6 (3.8 billion kg/year), causing the riverbed elevation to rise. Furthermore, substantial sedimentation has caused the riverbed to move and shrink, greatly reducing the flow area and flow capacity in the main channel. However, the effect of sediment concentration on flow capacity is correlated with inflow and the sediment transport rate. Under a high flow or sediment transport rate, even in high sediment concentration conditions, the amount of silt in the channel will not increase, whereas the flow capacity will increase. By contrast, under low flow or sediment transport rate conditions, the amount of silt in the channel will increase, whereas the flow capacity will decrease with a high sediment concentration.

Fig. 10 shows the typical cross-section morphology for the Ningxia-Inner Mongolia reach. Fig. 10 depicts two production dikes at the center of the riverbank. The river is not allowed to overflow in this area for farmland and settlements, which greatly reduces the channel's flow area. Moreover, many areas in the channel are used for crop planting and house building when the water flow in the river is small, which also reduces the flow capacity. Additionally, some dikes are constructed without professional planning, design, and construction. Such dikes do not meet flood-control standards, are noncontinuous, and cannot perform the required functions of a standardized dike to defend against medium and small-scale flooding. Overall, inadequate production, inadequate standards, and weak dikes reduce the flow area and directly reduce flow capacity.

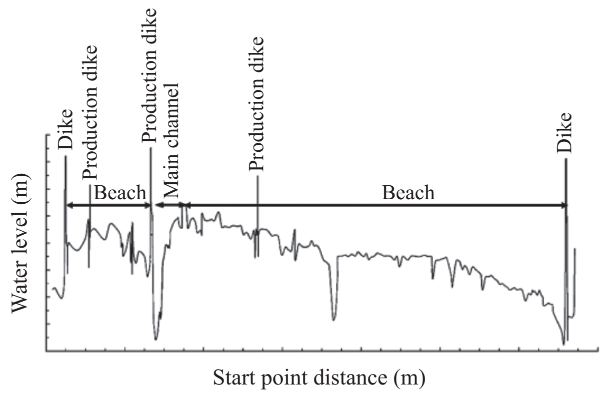

Fig. 10. Typical cross-section morphology of the Ningxia–Inner Mongolia reach.

IV. METHODOLOGY

1. Modeling

Because of reduced inflow and rising water demand, less water is available from the Yellow River, causing the water level to fall and the flow to decrease. Additionally, sedimentation and below-standard dikes reduce the flow area and flow capacity, increasing the likelihood of flooding. We present a flow-capacity model in this paper to illustrate the overflow conditions and rapidly and efficiently increase the flow capacity of the channel.

As discussed, dikes are a key cause of reduced flow capacity. Thus, we propose a flow-capacity model (Fig. 6) based on the standardized dikes along the studied river stretch.

Using standardized dikes means no dikes or other obstructions are constructed on riverbank. In particular, standardized dikes must comply with the Design Specifications of the Dike Project of China (GB50286-1998), and they are constructed at four standard levels along the entire river to protect against flood of 20-30 year return period.

By using a standardized dike, the relationships between various water levels and corresponding flows for each section can be determined. Once the water level of a channel, bankfull, and dike are determined, a flow-capacity model can be established as follows:

$$Q_{flow,i} = f(Z_{c,i}, Z_{b,i}, Z_{d,i}) \quad (1)$$

where $Q_{flow,i}$ is the flow capacity of section i; $Z_{c,i}$ is the water level of the channel in section i, which corresponds to maximum channel flow; $Z_{b,i}$ is the water level of the bankfull in section i, which corresponds to the maximum bankfull flow; and $Z_{d,i}$ is the safe water level of the dike in section i, which corresponds to the maximum safe flow in section i. Flow between the water level of the channel and bankfull is the so-called overbank flow.

The river flow capacity is closely related to velocity. In this paper, velocity affects the safe water level of a dike because the velocity has a negative influence on dike erosion. Thus, the safe water level of a dike can be appropriately determined using the maximum velocity.

2. Methods

Section-flow estimates include two parts: (1) determining the corresponding water level, flow area, velocity, width, and depth and (2) estimating the section flow on the basis of the water level or related relationships between the water level and section flow. The commonest methods used to estimate section flow include: (1) water-level and flow-relationship curves (Leopold et al., 1964); (2) the hydraulic geometric characteristics of a typical cross-section with velocity-flow area relationships or the velocity-area method (Harman et al., 2008); and (3) the Manning resistance equation (Harman et al., 2008). In this study, these three methods are referred to as MD1, MD2, and MD3, respectively. Therefore, this study focuses on maximum discharge and water-level estimation instead of bankfull-discharge estimation (Xia et al., 2009), bankfull-discharge magnitude and frequency (Navratil et al., 2006), or section-flow capacity, which can be calculated by using both bankfull discharge and maximum safe discharge based on the maximum safe water level of a dike. In this study, the three aforementioned methods are used to establish the flow-capacity models.

MD1: Water Level and Flow Relationships

On the basis of the daily water level and flow data, water level and flow relationships can be established by fitting a special curve. However, if the cross-section morphology remains relatively stable, water-level and flow-relationship curves can be effective and useful for estimating section flow. When the available data timescales are small, the water-level and flow-relationship curves will be more useful. Additionally, flood-event data are used to fit the water-level and flow-relationship curves (Xia et al., 2009). If data on high water levels or flow are unavailable, then the flow-relationship curve can be extended on the basis of its own characteristics. If the water level is determined, then the corresponding flow can be estimated as

$$Q'_{flow,i} = f(Z_i, f(Z_i \sim Q_i)) \tag{2}$$

where Z_i is the water level of section i, Z_i~Q_i is the water-level and flow-relationship curve of section i, and $Q'_{flow,i}$ is the corresponding flow of section i, by MD1.

MD2: Velocity-Area Method

Each section's flow processes are measured annually using a velocity instrument. The flow-process data, including water level, flow, water surface area and width, water depth, and flow velocity, are presented in Table 1. On the basis of these data, the corresponding average velocity of the cross-section flow can be obtained. On the basis of the latest stable cross-section morphology, the velocity-area or flow area-velocity can be plotted. Similarly, if data on high water levels, widths, and depths are unavailable, the relationship curves can be extended on the basis of their own characteristics or trends. When the bankfull water level or maximum water level is determined, the corresponding flow can be calculated by multiplying the width, depth, and velocity or the flow area and velocity:

$$\begin{aligned} Q''_{flow,i} &= f(v_i, h_i, l_i) \\ &= \sum_{i=1}^{n}\left(\frac{v_i + v_{i+1}}{2}\cdot\frac{h_i + h_{i+1}}{2}\cdot l_{i+1}\right) \end{aligned} \tag{3}$$

or

$$Q''_{flow,i} = \int_1^n v_i dA_i = \int_1^n v_i \cdot h_i dl_i \quad i \in [1, n], \tag{4}$$

where, v_i, h_i, and l_i are the average flow velocity, water depth, and water surface width of section i, $f(v_i, h_i, l_i)$ is the velocity-area method curve of section i, A_i is the flow area of section i, and $Q''_{flow,i}$ is the corresponding flow of section i based on MD2.

MD3: Manning Resistance Equation

Another widely used flow-equation method for flow (or discharge) is the Manning resistance equation (Kartezhnikova and Ravens, 2014):

$$\begin{aligned} Q'''_{flow,i} &= \frac{1}{n}\cdot R_{n,i}^{2/3}\cdot S_i^{1/3}\cdot\int_1^n h_i dl_i \\ &= \frac{1}{n}\cdot R_{n,i}^{2/3}\cdot S_i^{1/3}\cdot\sum\left(\frac{h_i + h_{i+1}}{2}\cdot l_{i+1}\right) \end{aligned} \quad i \in [1, n], \tag{5}$$

where n is the Manning roughness coefficient (s/m$^{1/3}$, gained from measured data), $R_{n,i}$ is the hydraulic radius of section i (m, flow area/wetted perimeter), and S_i is the slope of section i. $Q'''_{flow,i}$ is the flow of section i as determined using MD3.

According to Table 1, A_i, h_i, and l_i can be obtained from the data on cross-section morphology, and the average values of v_i are measured annually. The Manning roughness coefficients are determined on the basis of flow, flow velocity, sediment concentration, and other factors; their values are between 0.015 and 0.050 in different sections (Zhang et al., 2012). $R_{n,i}$ can be calculated using the morphology data as well as the flow area and wetted perimeter.

V. RESULTS AND DISCUSSION

In this paper, the flow capacities based on standardized dikes in each section are estimated using MD1, MD2, and MD3.

Table 4. Design of standardized dike (part).

Stake number	Crest Elevation (m)	Width of dike (m)	Designed Water level (m)	Designed ultrahigh (m)	Slope of dike Near river	Slope of dike Back river	Ground elevation Near river (m)	Ground elevation Back river (m)
1+500	1056.47	6.0	1053.30	1.6	1:3	1:3	1054.44	1051.44
10+500	1053.61	6.0	1051.75	1.6	1:3	1:3	1050.48	1050.48
20+500	1051.98	6.0	1049.70	1.6	1:3	1:3	1048.06	1048.06
30+500	1050.39	6.0	1048.73	1.6	1:3	1:3	1047.60	1045.90
40+000	1048.77	6.0	1047.21	1.6	1:3	1:3	1049.71	1046.00
50+000	1046.57	6.0	1044.91	1.6	1:3	1:3	1043.14	1042.37
60+000	1045.05	6.0	1043.05	1.6	1:3	1:3	1041.69	1041.37
70+000	1043.16	6.0	1040.86	1.6	1:3	1:3	1039.04	1038.50
80+000	1041.21	6.0	1039.13	1.6	1:3	1:3	1036.74	1037.61
…	…	…	…	…	…	…	…	…

Note: Designed water level is the maximum safe water level of the dike.

Table 5. Flow estimation performance by method and section.

	S3				S5				S6			
	MRE	RMSE	MAE	CC	MRE	RMSE	MAE	CC	MRE	RMSE	MAE	CC
MD1	0.070	10.6	1.12	0.99	0.040	5.9	0.65	0.99	0.041	19.06	2.2	0.99
MD2	0.182	31.4	3.31	0.99	0.123	15.3	1.69	0.99	0.145	81.15	9.2	0.99
MD3	0.105	27.2	2.86	0.99	0.083	32.0	3.53	0.99	0.079	39.23	4.4	0.99

Table 6. Present flow capacity and flow capacity based on standardized dike.

	Present flow/flow based on standardization dike (m^3/s)								
	Max channel water level/bankfull water level (m)						Max safety water level of dike (m)		
	S3	S5	S6	S3	S5	S6	S3	S5	S6
	1088.4	1019.6	988.0	1094.0	1023.4	992.8	1096.8	1026.2	995.6
MD1	1920	1670	1380	6580	5890	5740	8920	9000	8290
MD2	2100	1470	1330	8150	7990	11990	11870	12740	14730
MD3	2000	1880	1320	7600	6630	5320	10400	12130	7650
Average	2007	1673	1343	7443	6837	7683	10397	11290	10233

as shown in Fig.11. First, the current cross-section morphology and water-level and flow-relationship curves for S3, S5, and S6 can be plotted on the basis of the measured start-point distance, elevation, flow, and water-level data (Data 3: 2011-2012). Second, we can characterize the relationships between (1) the flow area and water level and (2) the flow velocity and water level. Third, data on partially standardized dikes constructed on the Ningxia-Inner Mongolia reach are collected and presented in Table 4, in which the bankfull water level, safe water level, and crest water level of dikes in each section is provided. Last, flow capacities are estimated for the various water levels by using MD1, MD2, and MD3.

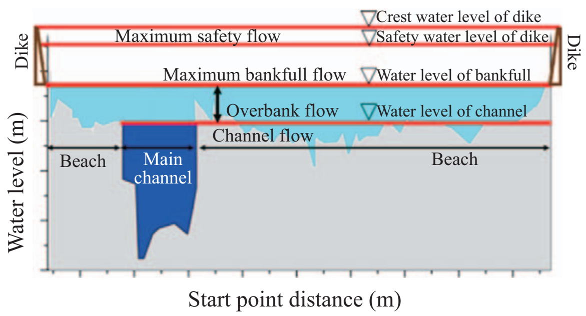

Fig. 11. Flow capacity analysis based on standardized dike.

To assess the methods' performance, comparison of the measured and estimated flow values derived using MD1, MD2, and MD3 is shown in Fig. 12, taking the flow estimates of S3, S5, and S6 from 2012 as examples. The correlation coefficient (CC), root mean square error (RMSE), mean absolute error (MAE), and mean related error (MRE) are used as criteria to assess the methods' performance. Estimated and measured flow values derived using MD1, MD2, and MD3 are compared in Table 5.

Flow capacity can currently be described by maximum channel-

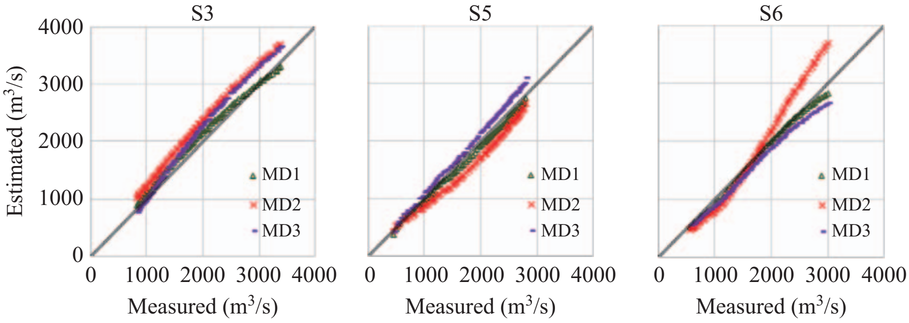

Fig. 12. Comparison of measured and estimated values of flow for 2012 using MD1, MD2, and MD3.

water level and bankfull water level, which are determined on the basis of the cross-section morphology. Flow capacity based on standardized dikes can subsequently be described by dike's designed water level (Table 4). Once the characteristic water level is ascertained, the section-flow capacity can be estimated using MD1, MD2, and MD3 (Table 6).

As shown in Fig. 12 and Table 6:

(1) The MRE of the three methods are all within ±20%, which meets the accuracy requirement, and the applicability and reliability of the three methods are verified;
(2) The three methods are accurate; the curves fit favorably, and all data points roughly agree;
(3) The comprehensive criteria employed in this study indicate that MD1 is consistently superior to MD2 and MD3 and flow-value estimates derived using MD1 are more accurate than those derived using MD2 or MD3. Thus, MD1 is recommended for describing the flow capacity of the upper Yellow River.

VI. CONCLUSION

In this paper, more than 440,000 data points are collected and divided into three independent sets: Data 1, Data 2, and Data 3. The reasons for reduced flow capacity in the past, including inflow, water supply, sedimentation, and dikes, are illustrated by comparing Data 1 and Data 2. The flow-capacity model established using Data 3 on the basis of standardized dikes is proposed in this paper, and flow capacities are estimated using three methods: MD1, MD2, and MD3.

Taking S3, S5, and S6 in 2012 as an example, the applicability and capability of the model and the accuracy of the three methods are verified. CC, RMSE, MAE, and MRE are selected to assess the methods' performance, and the data demonstrate that although estimated flow derived using all three methods can meet the accuracy requirements. MD1 is consistently superior to MD2 and MD3 and is recommended for estimating section-flow capacity.

In general, a flow-capacity model based on standardized dikes provides accurate and reliable estimated flows, where the values of CC exceed 0.99. The current maximum bankfull flows of S3, S5, and S6 are 6,670 m^3/s, 6,890 m^3/s, and 6,240 m^3/s, respectively, according to MD1. By using standardized dikes, the maximum flow of S3, S5, and S6 can be increased to 8,920 m^3/s, 9,000 m^3/s, and 8,290 m^3/s, respectively, according to MD1, which lays a solid foundation for water and sediment regulation in the Ningxia-Inner Mongolia reach. Our research results have practical significance for improving the overflow conditions of the Ningxia-Inner Mongolia reach and accelerating the construction process of standardized dikes along the Yellow River.

ACKNOWLEDGEMENTS

This study is supported by the National Key R & D Program of China (2017YFC0405900); Planning Project of Science and Technology of Water Resources of Shaanxi (2017slkj-16, 2017slkj-27); the China Postdoctoral Science Foundation (2017M623332XB); and the Basic Research Plan of Natural Science in Shaanxi Province (2018JQ5145). The authors are indebted to the reviewers for their valuable comments and suggestions.

REFERENCES

Azamathulla, H. M. and A. Zahiri (2012). Flow prediction in compound channels using linear genetic programming. Journal of Hydrology 454, 203-207.
Bai, T., Y. B. Kan, J. X. Chang, Q. Huang and F. J. Chang (2017). Fusing feasible search space into PSO for multi-objective cascade reservoir optimization. Applied Soft Computing 51, 328-340.
Chang, J., T. Bai, Y. M. Wang and Q. Huang (2012). Discussion on water and sediment regulation of desert valley reaches upper the Yellow River. Special issue of water resources reasonable allocation and optimal operation techniques in 2012, Water Conservancy Technical Information Center of China, Shaanxi, Xi'an, 121-127.
Chen, X. J., Q. W. Han and C. M. Fang (2007). Variation of dominant flow in Lower Yellow River and its influence on river channel. Journal of Hydraulic Engineering 38(1), 15-22.
Chang, F. J. and K. W. Wang (2013). A systematical water allocation scheme for drought mitigation. Journal of Hydrology 507, 124-133.
Emiroglu, M. E., N. Kaya and H. Agaccioglu (2010). Flow capacity of labyrinth side weir located on a Straight Channel. Journal of Irrigation and Drainage Engineering 136(1), 37-46.
Emiroglu, M. E., O. Kisi and O. Bilhan (2010). Predicting discharge capacity of triangular labyrinth side weir located on a straight channel by using an adaptive neuro-fuzzy technique. Advances in Engineering Software 41(2), 154-160.
Fu, G. B., S. L. Chang, C. M. Liu and D. Shepard (2004). Hydro-climatic trends of the Yellow River Basin for the last 50 years. Climatic Change 65(1), 149-178.

Harman, C., M. Stewardson and R. DeRose (2008). Variability and uncertainty in reach bankfull hydraulic geometry. Journal of Hydrology 351, 13-25.
Kordi, E. and I. Abustan (2011). Estimating the overbank flow using slope-area method. Journal of Hydrologic Engineering 16(11), 907-913.
Kartezhnikova, M. and T. M. Ravens (2014). Hydraulic impacts of hydrokinetic devices. Renewable Energy 66, 425-432.
Leopold, L. B., G. M. Wolman and J. P. Miller (1964). Fluvial processes in geomorphology. W.H. Freeman and Co., San Francisco, CA.
Navratil, O., M.B. Albert, E. Hérouin and J. M. Gresillon (2006). Determination of bankfull discharge magnitude and frequency: comparison of methods on 16 gravel-bed river reaches. Earth Surf. Process. Landforms 31, 1345-1363.
Ran, L. S., S. J. Wang and X. L. Fan (2010). Channel change at Toudaoguai station and its responses to the operation of upstream reservoirs in the upper Yellow River. Journal of geographical sciences 20(2), 231-247.
Tayfur, G. and V. P. Singh (2011). Predicting mean and bankfull discharge from channel cross-sectional area by expert and regression methods. Water Resources Management 25(5), 1253-1267.
Unal, B., M. Mamak, G. Seckin and M. Cobaner (2010). Comparison of an ANN approach with 1-D and 2-D methods for estimating flow capacity of straight compound channels. Advances in Engineering Software 41(2), 120-129.
Unes, F., D. Joksimovic and O. Kisi (2015). Plunging flow depth estimation in a stratified dam reservoir using neuro-fuzzy technique. Water Resources Management 29(9), 3055-3077.
Wu, B. S., Y. F. Zhang and J. Q. Xia (2008). Variation of bankfull area at Gaocun station in the Lower Yellow River. Journal of Sediment Research 2, 34-40.
Xia, J. Q., B. S. Wu, Y. P. Wang and W. W. Li (2010). Estimating the bankfull flow in the Lower Yellow River and analysis of its variation processes. Journal of Sediment Research 2, 6-14.
Xia, J. Q., B. S. Wu and W. W. Li (2009). Comparison of different approaches to determine bankfull discharge in the Lower Yellow River. Journal of Sediment Research 3, 20-29.
Xu, Z. X., K. Takeuchi, H. Ishidaira and X. W. Zhang (2002). Sustainability analysis for Yellow River Water Resources using the system dynamics approach. Water Resources Management 16(3), 239-261.
Zhang, L. H. (2012). Reasons for the abnormal channel roughness of the Yellow River and the solution to its problems. Journal of Hydraulic Engineering 43(11), 1261-1270.